Photoinduced electron transfer from conjugated polymers to CdSe nanocrystals

D. S. Ginger and N. C. Greenham
Cavendish Laboratory, Madingley Road, Cambridge, CB3 0HE, United Kingdom
(Received 27 October 1998)

We study photoinduced electron transfer from derivatives of poly(*p*-phenylenevinylene) (PPV) and nanocrystals of cadmium selenide via photoluminescence (PL) quenching and photoinduced absorption (PIA) spectroscopy. Using size-dependent quantum confinement to vary the energy levels of the nanocrystal acceptors, and chemical substitution to vary the energy levels of the polymer donors, we present a systematic investigation of charge transfer in these polymer/quantum-dot composites. We observe efficient PL quenching in blends of poly[2-methoxy-5-(2′-ethyl-hexyloxy-*p*-phenylenevinylene)] (MEH-PPV) with nearly monodisperse CdSe samples for nanocrystal diameters from 2.5 to 4.0 nm. The observed PIA peaks, as well as their frequency and temperature dependence, are consistent with the formation of long-lived positive polarons on MEH-PPV following electron transfer to the nanocrystals. Both the PL quenching and the PIA features are insensitive to nanocrystal size. We have also studied blends of CdSe nanocrystals of 2.5–4.0 nm diameter with two high electron affinity cyano-substituted PPV derivatives. One of these polymers behaves similarly to MEH-PPV; however in the other polymer, which has different alkoxy side chains, we find neither efficient PL quenching nor any PIA features indicative of charge transfer. We explain the insensitivity of the electron transfer process to nanocrystal size in the context of the relevant polymer and nanocrystal energy levels and discuss the influence of the polymer side chains on the charge-transfer process. [S0163-1829(99)13215-6]

I. INTRODUCTION

Photoinduced charge separation is a process of central importance in the field of polymeric semiconductors: its study not only contributes to our understanding of the basic photoexcited states in these ''one-dimensional'' semiconductors, but is also of technological importance in the development of efficient nonlinear optical[1,2] and photovoltaic devices.[3–5] Conjugated polymers are a class of materials that show great promise in these areas, both because they can easily be processed to form large-area devices and because their energy gaps and ionization potentials can readily be altered by chemical modification of the polymer chain. Despite this promise, single-layer polymer devices generally exhibit a low efficiency in converting incident photons into electrical charges. This is because the dominant photogenerated species in most conjugated polymers is a neutral exciton. Since these neutral excitations can be dissociated at an interface between the polymer and an electron accepting species, charge separation is often facilitated via inclusion of a high electron affinity substance such as C_{60} (Refs. 5 and 6) or a cyano-substituted polymer.[3,7] Common features of all such successful charge-separation-enhancing materials include both an electron affinity high enough to make charge transfer energetically favorable and the ability to form blends with morphologies that allow a high percentage of the excitons to encounter an interface within their typical diffusion range of 5–10 nm.[6] In addition, the charge-separation process must be fast enough to compete with the radiative and nonradiative decay pathways of the singlet exciton, which typically occur on time scales of 100–1000 ps.[8] Another class of electron acceptors with the potential to fulfill these requirements, nanocrystalline inorganic semiconductor particles, has received recent attention,[9,10] partly as a result of the report by O'Regan and Grätzel of efficient solar cells based on organic-dye-sensitized nanocrystalline TiO_2 particles.[11]

Semiconductor nanocrystals, like conjugated polymers, represent a class of low dimensional compounds with interesting optical, electronic, and physical properties.[12–14] Nanocrystals have an exceptionally large surface area to volume ratio when compared with bulk materials. This property has received much attention in the study of TiO_2 nanocrystal/polymer composites because it provides a remarkable amount of internal surface area at which charge transfer can occur. When the size of the nanocrystal is smaller than that of the exciton in the bulk semiconductor, the lowest energy optical transition is significantly blueshifted due to quantum confinement. Because the chemical synthesis of II-VI semiconductors such as CdSe can produce monodisperse samples of various sized nanocrystals,[15,16] quantum confinement effects can be used to tune the optoelectronic properties, including both band gap and electron affinity, of the resulting semiconductor quantum dots. This is particularly useful for the study of photoinduced charge separation in composites.[10] For CdSe nanocrystals, which can be prepared with diameters in the 6–2-nm range, the optical gap can conveniently be tuned through a large part of the visible spectrum (from 2–2.6 eV). Recently, it has also been shown that nanocrystals of CdSe can act as efficient electron acceptors when blended with the semiconducting polymer MEH-PPV, yielding photovoltaic devices with quantum efficiencies of up to 12%.[9]

The use of CdSe nanocrystals as electron acceptors in polymer blends provides unique advantages to the study of photoinduced charge separation. Because the nanocrystal surfaces can be modified through the addition or removal of organic ligands without altering the intrinsic electronic properties of the nanocrystals, there exists the possibility to alter the blend morphology or to introduce a controlled spatial barrier to charge transfer while still retaining the size-tunable

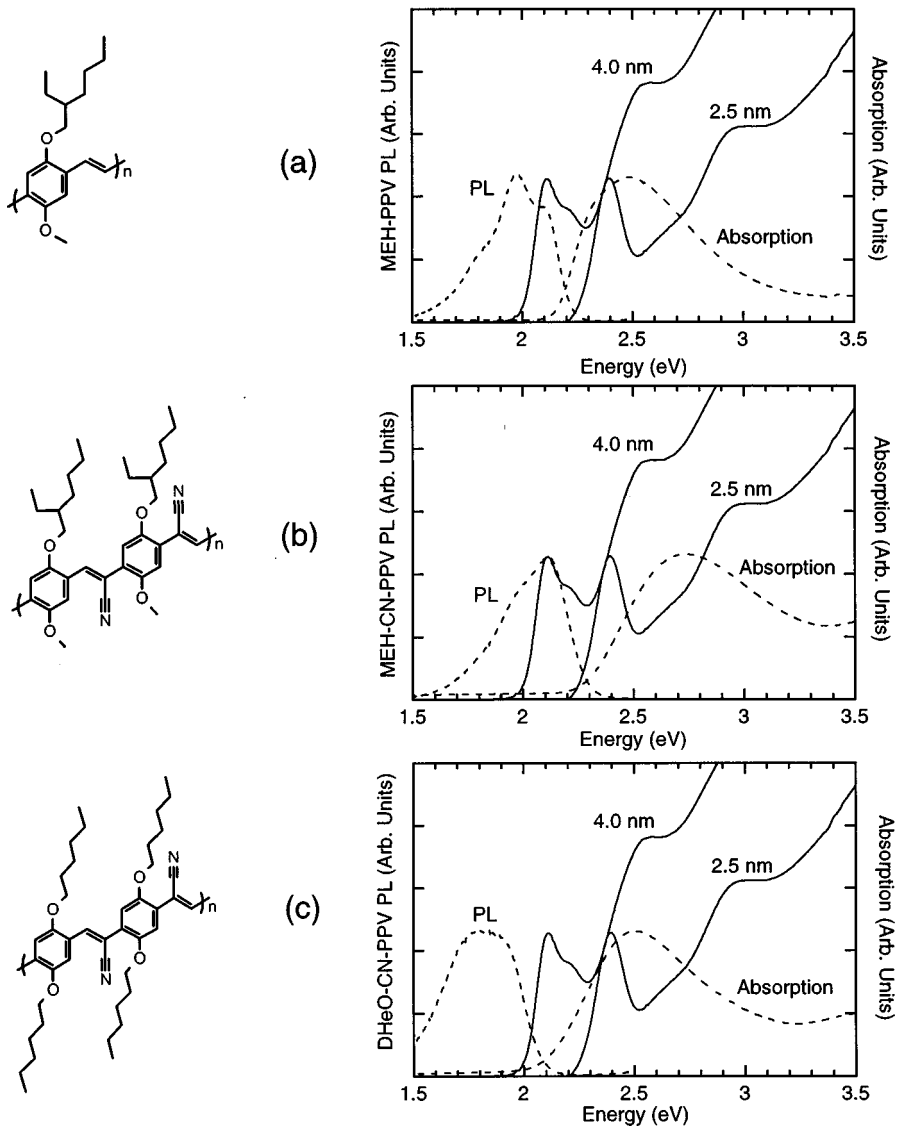

FIG. 1. Structures of the polymers used in these experiments, (a) MEH-PPV, (b) MEH-CN-PPV, (c) DHeO-CN-PPV, along with the photoluminescence (PL) and absorption spectra of the polymers (dashed lines), overlaid with the absorption spectra of the 4.0- and 2.5-nm-diameter nanocrystals (solid lines).

properties of the quantum dots. Perhaps more importantly, because the energy levels of the host polymers can be tuned through chemical derivatization of the backbone chains, and the energy levels of the nanocrystals can be tuned through size-dependent quantum confinement effects, blends of the two materials offer the possibility of careful and independent positioning of both donor and acceptor levels.

In the present study we have explored a systematic series of conjugated polymer/nanocrystal composites based on the three polymers MEH-PPV, DHeO-CN-PPV, and MEH-CN-PPV (Fig. 1), blended with a size-selected series of 2.5-, 3.3-, and 4.0-nm-diameter CdSe nanocrystals. Photoluminescence (PL) quenching measurements and steady-state photoinduced absorption (PIA) spectroscopy have been used to detect and characterize the charge-transfer process in these composites and the morphologies of the blends have been examined by transmission electron microscopy (TEM).

II. EXPERIMENT

The structures of the polymers used, MEH-PPV, DHeO-CN-PPV, and MEH-CN-PPV, are shown in Fig. 1. All three polymers were used as received and dissolved in chloroform. Nearly monodisperse samples of CdSe nanocrystals were synthesized by the tri-*n*-octylphosphine-oxide (TOPO) method of Murray *et al.*,[15] as modified by Katari and co-workers.[16] The TOPO surface ligand was removed from the CdSe samples by washing the nanocrystals three times with methanol and then three times dissolving them in the minimum quantity of pyridine and precipitating them with hexanes. Displacement of the surface ligand with pyridine is expected to remove approximately 90% of the TOPO originally bound to the surfaces,[16,17] and has been shown to increase charge separation efficiency at polymer/CdSe interfaces.[9] The final nanocrystal precipitate was dissolved in chloroform without drying. Both nanocrystal and polymer

solutions were filtered with 0.5 μm PTFE filters. Solution concentrations were subsequently determined by evaporating known volumes to dryness and then weighing. Solutions were mixed to obtain the desired weight ratios of nanocrystal to polymer and then films were obtained by spin coating in a nitrogen dry box at approximately 2000 rpm. PL efficiencies were measured under nitrogen flow using an integrating sphere, as described elsewhere.[18] Excitation for the PL measurements was provided by an argon-ion laser operating as near to the polymer absorption maximum as possible (either 458 or 488 nm) with a power of approximately 1 mW.

PIA measurements were performed with the samples mounted in a helium flow cryostat fitted with a heating element and temperature controller. Temperature was monitored separately with a calibrated Si diode located near the sample. The experiments used standard phase-sensitive techniques with a mechanically chopped argon-ion laser operating at 458 or 488 nm as the excitation source. Typical laser intensity was approximately 20 $\mathrm{mW\,cm^{-2}}$. Detection was provided by a silicon photodiode, or a liquid nitrogen cooled InAs photodiode, depending on the wavelength range (500–1000, and above 1000 nm, respectively). Fractional photoinduced changes in the sample transmittance ($\Delta T/T$) were monitored as a function of wavelength using a lock-in amplifier. The phase of the lock-in amplifier was set so that the polymer PL signal, which occurs on a time scale of less than 1000 ps, appeared entirely as a positive signal in the X (in-phase) channel. Induced absorptions due to long-lived excited states thus appeared as a negative signal in the X channel accompanied by a positive signal in the Y (90° out-of-phase) channel. In the data presented here, the PL signal has been subtracted by measuring it separately from the PIA signal at each wavelength. Samples were kept at all times in either an inert atmosphere or under dynamic vacuum, to avoid photo-oxidation.

Transmission electron microscopy (TEM) was performed on very thin films (approximately 10–20 nm) using a JEOL-2000 microscope operating at 200 kV. Films were prepared by spin coating onto glass slides, scoring the films, and then floating them onto the surface of a water bath. The films were then transferred to holey carbon grids for measurement.

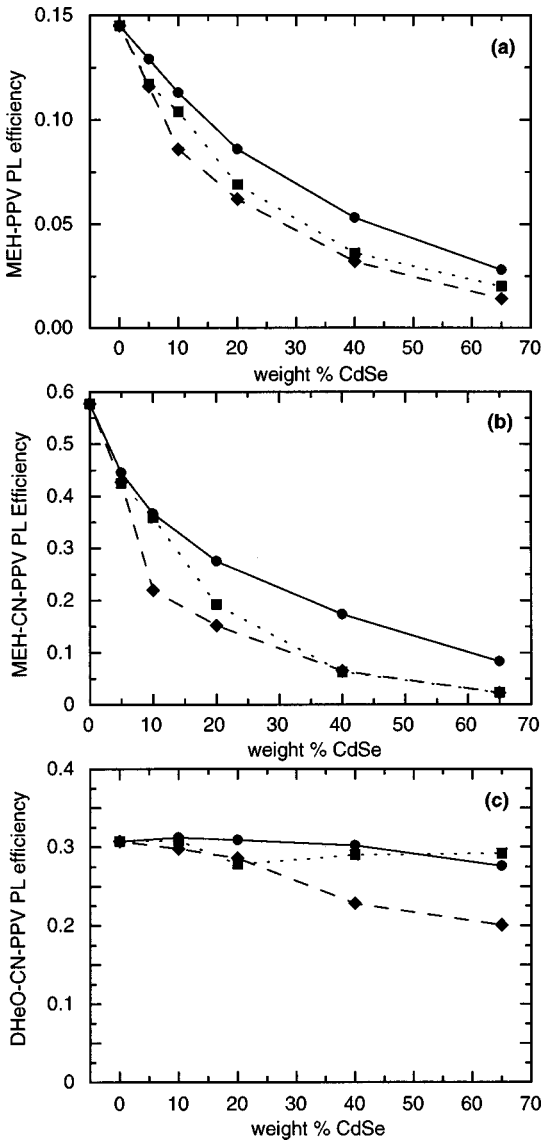

FIG. 2. Photoluminescence efficiencies of blends of (a) MEH-PPV, (b) MEH-CN-PPV, and (c) DHeO-CN-PPV with CdSe nanocrystals of 2.5 (squares), 3.3 (circles), and 4.0 (diamonds) nm in diameter.

III. RESULTS AND DISCUSSION

A. Photoluminescence quenching

Figure 2 shows the PL efficiency of CdSe nanocrystal/conjugated polymer composites with nanocrystal diameters of 2.5, 3.3, and 4.0 nm. With MEH-PPV and MEH-CN-PPV there is significant quenching of the PL with increasing nanocrystal concentration. With DHeO-CN-PPV, however, the quenching is much less pronounced, especially for the smaller nanocrystal sizes.

PL quenching provides evidence for charge transfer, because once the singlet exciton has been dissociated, it can no longer decay radiatively to the ground state. Indeed, PL quenching with MEH-PPV and 5-nm-diameter CdSe nanocrystals was observed previously,[9] and was attributed to charge transfer at the polymer/nanocrystal interface. Here, we observe similar behavior over an entire size series of decreasing diameter nanocrystals. Although we expect the smaller nanocrystals to possess lower electron affinities due to quantum confinement, these data indicate that the electron affinity of even the smallest CdSe nanocrystals is sufficient to allow electron transfer from MEH-PPV. This interpretation is supported by an examination of the electron affinities (EA's) of both the polymer and the nanocrystal.

Charge transfer from polymer to nanocrystal will be energetically favorable if

$$E^{A}_{\text{nanocrystal}} - E^{A}_{\text{polymer}} > U_{\text{polymer}} - V_{\text{charge transfer}}, \qquad (1)$$

where U_{polymer} is the Coulombic binding energy of the singlet exciton on the polymer and $V_{\text{charge transfer}}$ is the Coulombic energy associated with attraction between electron and hole in the final, charge-separated state. In general, we expect U_{polymer} to be significantly larger than $V_{\text{charge transfer}}$, due to the increased average electron-hole separation in the charge-separated state.

For the nanocrystals, we extrapolate from the bulk cadmium selenide EA of 4.87 eV (Ref. 19) and use the effective-mass approximation[20] to estimate that 80% of the experimentally observed band-gap shift occurs in the conduction band. This yields nanocrystal EA's in the range of 4.4–4.7 eV for nanocrystal sizes of 2.5–5 nm. The negative polaron level in MEH-PPV has been estimated at 3.0 eV via electroabsorption measurements.[21] Although only approximate, the calculated difference in EA's of 1.4–1.7 eV clearly provides a significant driving force for electron transfer from the polymer to nanocrystals of any size. There is still considerable controversy as to the magnitude of the Coulombic binding energy of the singlet exciton in PPV and its derivatives, but we note that even a binding energy as large as 1 eV would be insufficient to prevent charge transfer. We therefore find the calculated difference in EA's to be consistent with the strong PL quenching that is observed for all CdSe nanocrystal sizes in MEH-PPV.

In DHeO-CN-PPV, the PL efficiency remains largely unaffected by the addition of nanocrystals. Cyano-substitution withdraws electron density from the conjugated backbone, increasing the EA of the polymer. However, the lack of PL quenching in the DHeO-CN-PPV composites is still difficult to understand in the context of the above discussion of relative EA's. DHeO-CN-PPV has an EA that has been measured by cyclic voltammetry to be roughly 0.5 eV larger than that of MEH-PPV.[22] Therefore, one would expect the nanocrystals to possess an EA that is at least 0.9 eV larger than that of the DHeO-CN-PPV polymer. In such circumstances one would expect charge transfer and PL quenching to occur, unless the exciton binding energy in DHeO-CN-PPV was extremely large. It is interesting to compare the DHeO-CN-PPV results with those found for MEH-CN-PPV, which shows strong PL quenching. As seen in Fig. 1, MEH-CN-PPV has the same cyano-substitution as DHeO-CN-PPV and is thus expected to have highest occupied molecular orbital (HOMO) and lowest unoccupied molecular orbital (LUMO) levels very close in energy to those of DHeO-CN-PPV. It is therefore clear that the lack of charge transfer from the DHeO-CN-PPV to the nanocrystals cannot be related solely to the cyano-substitution of the polymer. The difference between MEH-CN-PPV and DHeO-CN-PPV is in the alkyl side chains that are used to confer solubility to the polymers, and we thus conclude that these side chains play an important role in the regulation of charge transfer. This conclusion is also consistent with the results of recent studies of photoexcitation dynamics in C_{60}/polymer blends.[23]

There are several possibilities as to the origin of the influence of the alkyl chains on the charge-transfer process. One possibility is their effect on phase separation: if the differing side chains resulted in large-scale phase separation (with nanocrystal and polymer domains much larger than the average exciton diffusion range), only a few excitons would be able to diffuse to the CdSe/polymer interfaces and be dissociated. The result would be minimal charge separation or PL quenching. The spin-coated films were of good optical quality, indicating no phase separation on the micron scale. To examine the structure of the blends on the nanometer scale, TEM was performed on blends of nanocrystals with both DHeO-CN-PPV and MEH-CN-PPV. The images in Fig. 3 show similar morphologies for DHeO-CN-PPV and MEH-CN-PPV. Variations in film thickness complicate any quantitative comparison of the images; however, for both types of polymer, the images show phase separation only on the nanometer scale, with typical domain sizes of tens of nanometers. Indeed, the images resemble those published earlier for blends of 5-nm-diameter CdSe nanocrystals with MEH-PPV.[9] We therefore discount the possibility that gross phase separation prevents excitons from being able to diffuse to a nanocrystal/DHeO-CN-PPV interface.

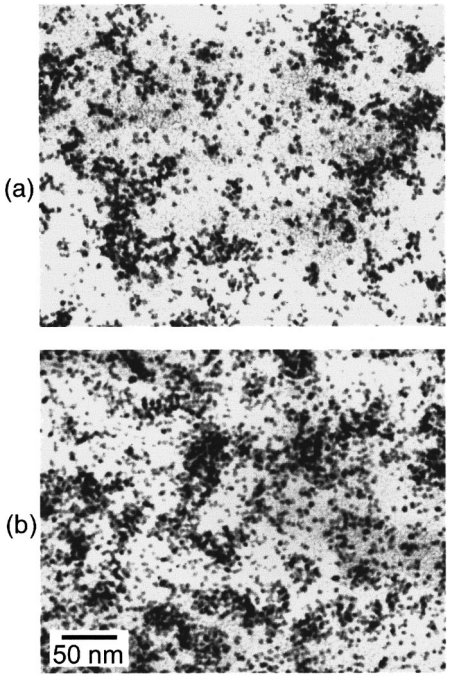

FIG. 3. TEM images of (a) MEH-CN-PPV and (b) DHeO-CN-PPV blended with 20% weight of 4.0-nm-diameter CdSe nanocrystals. Film thicknesses are 10–20 nm.

In Fig. 2, we have shown the PL as a function of nanocrystal concentration by weight (rather than by number density), and we find that the shape of the curves is not strongly dependent on nanocrystal size. This choice is based on the morphology observed in the TEM, which shows that the nanocrystals are aggregated rather than dispersed. It is therefore the weight or volume fraction of nanocrystals present that determines the quenching behavior, rather than the number of nanocrystals per unit volume.

A second possible reason for the lack of charge transfer from DHeO-CN-PPV is related to interchain interactions. It has been shown that in cyano-substituted polymers and oligomers with symmetric alkoxy side chains, close interchain spacing can lead to the delocalization of excitons across several chains.[24] In the solid state, this formation of lower energy interchain excitons has been observed on picosecond time scales.[25,26] It is therefore likely that many excitons delocalize before they diffuse to a polymer/nanocrystal interface. If the added stability of the interchain species were sufficient to prevent charge transfer, the effects of interchain spacing would explain the lack of PL quenching in the DHeO-CN-PPV blends. A large Stokes shift and a lack of vibronic structure in the emission are both commonly associated with interchain excitons,[24,26] and are both features

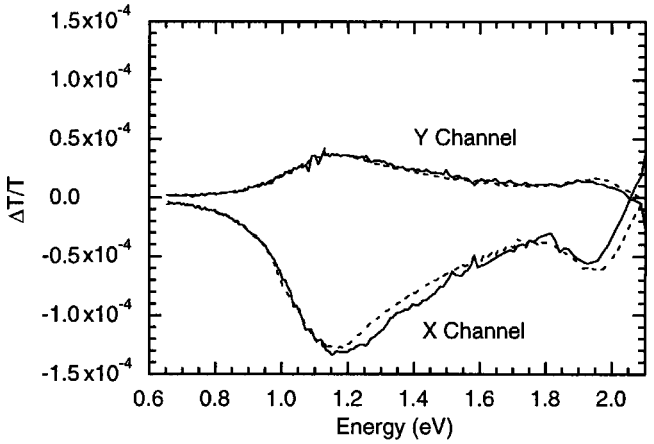

FIG. 4. PIA spectra of pristine DHeO-CN-PPV (dashed line) and a 40% weight 4.0-nm-diameter CdSe nanocrystal blend with DHeO-CN-PPV (solid line), both measured at 10 K. The upper two curves (positive $\Delta T/T$) are the *Y*-channel components of the signals, while the lower two (negative $\Delta T/T$) are the *X*-channel components.

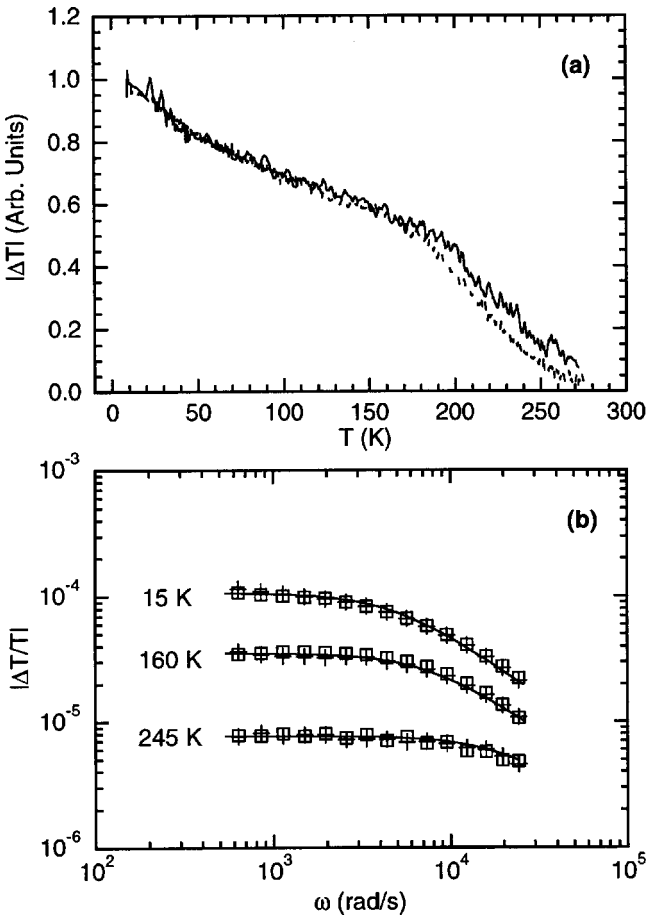

FIG. 5. (a) Temperature dependence of the PIA signal for pristine DHeO-CN-PPV (dashed line), and a 40% weight 4.0-nm-diameter nanocrystal blend with DHeO-CN-PPV (solid line). (b) Frequency dependence of DHeO-CN-PPV (squares) and the DHeO-CN-PPV/nanocrystal blend (crosses) at 15, 160, and 245 K, as indicated in the figure. The solid lines at each temperature represent fits of Eq. (2) to the data, with $\tau = 0.21$, 0.13, and 0.05 ms as discussed in the text. The data and fits have been offset for clarity by a factor of $\frac{1}{2}$ for the two warmer temperatures.

more strongly evident in DHeO-CN-PPV than in MEH-CN-PPV, indicating that interchain interactions are much more important in DHeO-CN-PPV. This provides a possible explanation for the difference in PL quenching behavior between the two polymers. However, the stabilization energy associated with interchain exciton delocalization is likely to be small compared with the difference in EA's driving the charge transfer, and is therefore unlikely to be sufficient to prevent charge transfer.

The final, and most likely, explanation for the lack of PL quenching in the DHeO-CN-PPV composites is that the presence of the dihexyloxy chains on both sides of the polymer prevents a nanocrystal from approaching sufficiently close to the conjugated backbone to allow charge transfer to occur. Although charge transfer is thermodynamically favorable, it is prevented from happening by a kinetic barrier. This is consistent with the fact that an 11 Å alkyl barrier surrounding CdS and CdSe nanocrystals, in the form of tri-*n*-octylphosphine oxide, is sufficient to prevent charge transfer.[9]

Finally, we note that where there is overlap between the polymer emission spectrum and the nanocrystal absorption spectrum (Fig. 1), there exists the possibility of Förster transfer of the exciton to the nanocrystal. This effect has been observed in polymer/nanocrystal blends before[9] and can lead to PL quenching, either through nonradiative decay in the nanocrystal or through subsequent hole transfer to the polymer. In DHeO-CN-PPV, we attribute the weak PL quenching observed with the largest nanocrystals to Förster transfer followed by nonradiative decay in the nanocrystals. This interpretation is supported below by our PIA measurements.

B. Photoinduced absorption (PIA) spectroscopy

The PIA spectra of pristine DHeO-CN-PPV and of a blend of DHeO-CN-PPV with CdSe nanocrystals are shown in Fig. 4, as measured at 10 K. Both samples show nearly identical PIA spectra over the range from 0.7 to 2.0 eV for both *X* and *Y* channels, with the main feature of the spectra being the large subgap absorption induced near 1.2 eV. Earlier PIA studies on DHeO-CN-PPV have attributed this peak to an absorption from a triplet exciton to a higher-lying triplet state.[27]

Because the triplet absorption commonly appears in the same spectral range as the polaron induced subgap absorptions in PPV derivatives, we also investigated both the temperature and frequency dependence of the 1.24 eV signal to determine if it was the product of only a single species. As shown in Fig. 5(a), the temperature dependence of the PIA signal at 1.24 eV was found to be identical for both samples in the range from 10 to 300 K. Figure 5(b) shows the frequency dependence of the 1.24 eV PIA signal in both DHeO-CN-PPV samples at temperatures 15, 160, and 245 K. As in Fig. 5(a), the behavior of the DHeO-CN-PPV and of the polymer/nanocrystal blend are identical.

The frequency dependence of the magnitude of the PIA signal, *S*, resulting from a single species undergoing monomolecular decay with a single lifetime τ is given by

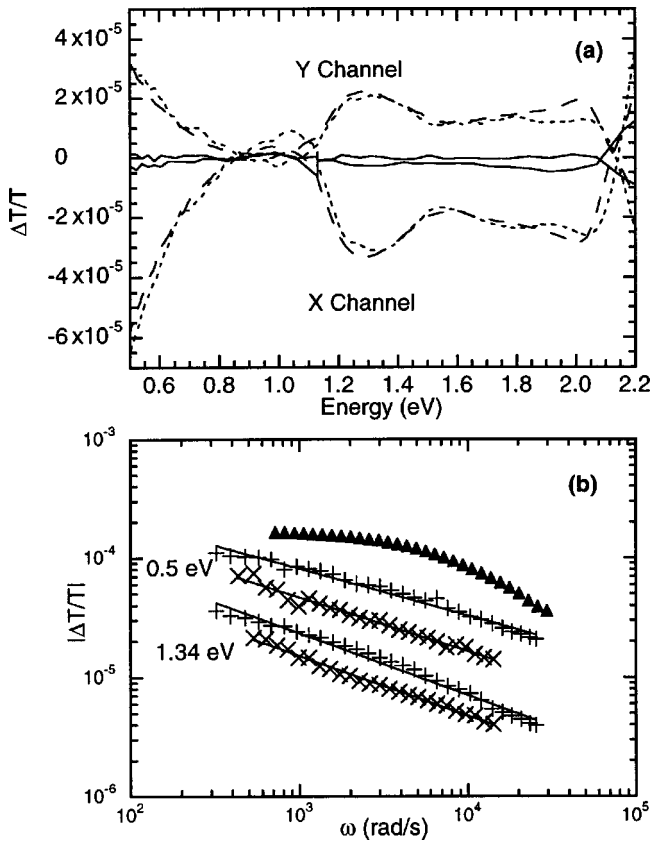

FIG. 6. (a) Room-temperature PIA spectra of MEH-PPV (solid line), a blend of MEH-PPV containing 40% weight of 4.0 nm CdSe nanocrystals (long dashes), and a blend of MEH-PPV and 40% weight of 2.5 nm CdSe nanocrystals (short dashes). (b) Frequency dependence of the 1.34 eV signal in pristine MEH-PPV at 10 K (triangles), along with that of the 0.5 and 1.34 eV features from the blend with 4.0 nm nanocrystals ($\times$) and the blend with 2.5 nm nanocrystals ($+$). The straight lines are power-law fits to the data, with exponents from -0.4 to -0.5.

$$S(\omega,\tau)=\frac{kI\tau}{\sqrt{1+\omega^2\tau^2}}, \tag{2}$$

where ω is the angular chopping frequency, I is the pump intensity, and k is a constant proportional to the absorption cross section of the species. The solid lines in Fig. 5(b) represent fits of Eq. (2) to the PIA data for DHeO-CN-PPV. The excellent agreement at all temperatures between the fits and the data for the pristine DHeO-CN-PPV and nanocrystal blends suggest that a single triplet species is indeed responsible for the observed PIA signal. The fits yield temperature-dependent triplet lifetimes of 0.21, 0.13, and 0.05 ms in DHeO-CN-PPV at the temperatures of 15, 160, and 245 K, respectively.

The absence of any additional PIA due to charge-separated states in the DHeO-CN-PPV sample containing nanocrystals, combined with the lack of efficient PL quenching in the nanocrystal/DHeO-CN-PPV blend, strongly suggest that electron transfer does not occur from this high electron affinity polymer to CdSe nanocrystals.

The room-temperature PIA spectra for pristine MEH-PPV and for blends with 2.5- and 4.0-nm-diameter nanocrystals are shown in Fig. 6(a). As expected, MEH-PPV shows no detectable PIA features at room temperature because of the strong temperature dependence of the triplet exciton lifetime. In contrast, both nanocrystal composites show several distinct features. These include a broad peak in the infrared near 1.3 eV, another in the visible at 2.0 eV, and a third peak beginning to grow in below 0.7–0.5 eV whose maximum is apparently too far into the infrared to be observed with our apparatus. Earlier PIA studies of C_{60}/MEH-PPV blends[2,28–30] allow us confidently to identify the peak at 1.3 eV, and the peak growing in below 0.5 eV, as the high-energy (HE) and low-energy (LE) features associated with charge on the polymer chain. Positive charge on the polymer leads to distortions of the conjugated backbone, generating self-localized polarons. These create the states within the π-π^* gap responsible for the LE and HE absorption features. The absorption near 2.0 eV has also been observed in PIA studies of MEH-PPV/C_{60} blends[29,30] where it has been termed the electroabsorption peak, because of its similarity to features seen in electroabsorption experiments.

If positive polarons on the polymer chain interacted strongly with the electrons on the nanocrystals, one might expect some modification of the PIA spectra depending on the size of the nanocrystals. As Fig. 6(a) shows, both the magnitude and position of the peaks are unchanged between the largest (4.0-nm-diameter) and smallest (2.5-nm-diameter) nanocrystals used in this study. We therefore do not find any evidence for an electron-polaron interaction that is affected by nanocrystal size.

The frequency dependence of the LE and HE signals at room temperature for both 2.5- and 4.0-nm nanocrystal/MEH-PPV blends is shown in Fig. 6(b). It is clear that the frequency dependence of the blend signals does not follow that expected for monomolecular decay kinetics. In the low-frequency limit ($\omega\tau \ll 1$), Eq. (2) predicts an absorption signal that is independent of frequency, while in the high-frequency limit ($\omega\tau \gg 1$), Eq. (2) yields a signal which is proportional to ω^{-1}. Although the functional form is more complicated, a similar frequency dependence is expected for bimolecular decay.[31] Instead, the observed signals exhibit an $\omega^{-0.5}$ dependence over the measured range from 100 to 4000 Hz. This $\omega^{-0.5}$ dependence has been reported before for polarons in PPV and its derivatives,[32] and deviations from single lifetime monomolecular and bimolecular decay have been observed in a recent study of sintered nanocrystalline TiO_2 and MEH-PPV.[33] In both instances the deviations have been attributed to the presence of a wide distribution of polaron lifetimes. We find that a distribution of five monomolecular decays is sufficient to exactly reproduce the $\omega^{-0.5}$ dependence over the range of frequencies covered in our experiments. Unfortunately, with so many free parameters a fit becomes degenerate. Nevertheless, from the $\omega^{-0.5}$ dependence from 100 to 4000 Hz, we can conclude that the lifetime distribution must at least include components longer than several ms, as well as components shorter than 100 μs.

The temperature dependence of the 1.34 eV PIA signal is shown for pristine MEH-PPV in Fig. 7(a). In the pristine polymer, no signal is observed above 150 K. However, below 150 K, a strongly temperature-dependent signal is seen that grows in strength with decreasing temperature. Both

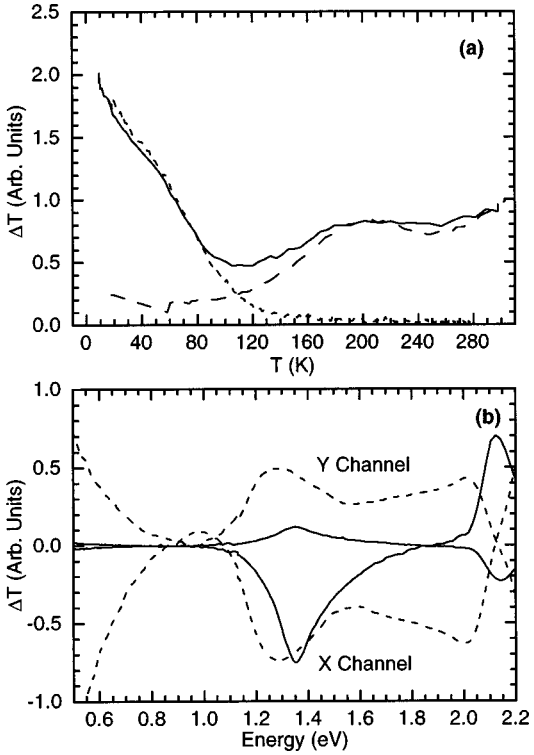

FIG. 7. (a) Temperature dependence of the PIA signals for MEH-PPV at 1.34 eV (short dashes) and for the MEH-PPV/40% weight 4.0 nm CdSe nanocrystal blend at 1.34 eV (solid line) and at 0.5 eV (long dashes). (b) PIA spectra observed in the MEH-PPV/40% weight 4.0 nm CdSe nanocrystal blend (solid line) at room temperature, next to the PIA spectra of pristine MEH-PPV at 10 K (the curves have been normalized so that their peak *X*-channel signals are equal).

from its strong temperature dependence and the shape of the spectra at 10 K [Fig. 7(b)], we can confidently assign the absorption centered at 1.3 eV to the triplet exciton seen in previous studies of MEH-PPV.[34]

Figure 7(a) shows the temperature dependence of the PIA signal in an MEH-PPV/nanocrystal blend at both 0.50 and 1.34 eV. At 0.50 eV, the signal is weakly temperature dependent, rising steadily in strength from 100 K up to 300 K, with a pronounced shoulder at 200 K. Since the triplet absorption is negligible at this energy, we identify this temperature dependence with that of the LE polaron feature. At 1.34 eV, in the low-temperature regime, the signal shows a temperature dependence which is nearly identical to that of the triplet in the pristine polymer. Above 120 K, however, the HE signal shows a component not present in the pristine polymer, which instead resembles the temperature dependence of the LE polaron feature. Because the HE signal occurs at the same energy as the main triplet-triplet absorption of the pristine polymer, it is clear that the signal observed at 1.34 eV is the sum of two components, the relative contribution of which depends on the temperature. At low temperatures it is dominated by the triplet absorption, while above 150 K the weakly temperature-dependent absorption due to the presence of polarons becomes dominant.

It is particularly interesting to note the increase in the strength of the polaron signal with increasing temperature. This increase could be the result of either a longer polaron lifetime or an increased generation rate. Because it is difficult to imagine a means by which the polaron lifetime would be enhanced as the temperature is raised, we conclude that the growth of the PIA signal at higher temperatures is due to an enhancement of the charge separation as the sample is warmed. However, the complex shape of the temperature dependence (with the shoulder at 200 K) suggests that both the polaron lifetime as well as the generation rate may be changing with temperature. Future studies may clarify this issue.

We note that the observation of triplet excitons in MEH-PPV/nanocrystal blends at low temperatures contrasts with the behavior observed in MEH-PPV/C_{60} blends, where the triplet signal is completely quenched.[29] The observation of a triplet signal in our blends implies that the typical time scale for charge separation is longer than the time scale for triplet exciton formation. Along similar lines, we note that the quenching of the PL in nanocrystal blends is much less complete than in C_{60} blends. This lack of complete quenching is consistent with the morphology of the nanocrystal blends described above, which show phase separation on the scale of tens of nanometers, compared with the typical exciton diffusion range of 5–10 nm.[6] A finite fraction of excitons may therefore undergo radiative decay or intersystem crossing before diffusing to a nanocrystal interface where charge separation may occur.

IV. CONCLUSIONS

We have explored photoinduced charge transfer in a series of conjugated polymer/CdSe nanocrystal composites. We have observed efficient charge separation leading to PL quenching in blends of nanocrystals with the polymers MEH-PPV and MEH-CN-PPV. We find that the efficiency of the charge separation is not sensitive to nanocrystal size, a result consistent with our estimates of the relative energy level placements between the polymers and the nanocrystals. Using PIA, we have observed long-lived positive polarons in blends in MEH-PPV and CdSe nanocrystals. We find a distribution of polaron lifetimes, spanning time scales less than 100 μs to greater than several ms, and find that the long-lived polaron states persist even at room temperature. In blends of DHeO-CN-PPV with CdSe nanocrystals, however, we have observed neither significant PL quenching nor any PIA signals associated with polarons, and we conclude that the symmetric dihexyloxy side chains of this polymer inhibit electron transfer to the nanocrystals. We have examined several possible causes for this behavior, and we suggest the arrangement of the alkyl side chains in DHeO-CN-PPV provides a spatial barrier which inhibits charge transfer. Furthermore, we find that the nanoscopic phase separation of the CdSe/polymer composites provides an important framework in which to interpret both the substantial, yet incomplete, PL quenching of the MEH polymers, as well as the coexistence of both triplet and polaron PIA features in various temperature regimes.

These results may be exploited in the rational design of nonlinear optical and photovoltaic devices based on nanocrystal/polymer composites. Because efficient charge

transfer is observed for all nanocrystal sizes, quantum confinement effects could be used to tune the properties of nanocrystal/polymer blends (i.e., to optimize voltage offsets, absorption maxima, or charge-transport properties), without adversely affecting charge separation. In a photovoltaic device based on a nanocrystal/polymer blend, recombination of polarons on the polymer with electrons on the nanocrystals represents the primary mechanism by which efficiency is lost. To achieve high efficiencies, the charge carriers must be extracted from the device before recombination can occur. The measurements of the time scale of this recombination process presented here thus provide important information for use in the design of photovoltaic devices.

ACKNOWLEDGMENTS

We thank V. M. Cleave, P. K. H. Ho, and B. A. Weir for experimental assistance, and Dr. S. C. Graham for valuable discussions. We thank the Melville Laboratory for Polymer Synthesis and Cambridge Display Technology for the supply of polymers.

[1] E. S. Maniloff, D. Vacar, D. W. McBranch, H.-L. Wang, B. R. Mattes, J. Gao, and A. J. Heeger, Opt. Commun. **141**, 243 (1997).
[2] E. K. Miller, K. Lee, K. Hasharoni, J. C. Hummelen, F. Wudl, and A. J. Heeger, J. Chem. Phys. **108**, 1390 (1998).
[3] J. J. M. Halls, C. A. Walsh, N. C. Greenham, E. A. Marseglia, R. H. Friend, S. C. Moratti, and A. B. Holmes, Nature (London) **376**, 498 (1995).
[4] G. Yu, J. Gao, J. C. Hummelen, F. Wudl, and A. J. Heeger, Science **270**, 1789 (1995).
[5] N. S. Sariciftci, L. Smilowitz, A. J. Heeger, and F. Wudl, Science **258**, 1474 (1992).
[6] J. J. M. Halls, K. Pichler, R. H. Friend, S. C. Moratti, and A. B. Holmes, Appl. Phys. Lett. **68**, 3120 (1996).
[7] G. Yu and A. J. Heeger, J. Appl. Phys. **78**, 4510 (1995).
[8] I. D. W. Samuel, B. Crystal, G. Rumbles, P. L. Burn, A. B. Holmes, and R. H. Friend, Chem. Phys. Lett. **213**, 472 (1993).
[9] N. C. Greenham, X. Peng, and A. P. Alivisatos, Phys. Rev. B **54**, 17 628 (1996).
[10] Y. Wang, N. Herron, and J. Caspar, Mater. Sci. Eng., B **19**, 61 (1993).
[11] B. O'Regan and M. Grätzel, Nature (London) **353**, 737 (1991).
[12] A. P. Alivisatos, Science **271**, 933 (1996).
[13] M. G. Bawendi, M. L. Steigerwald, and L. E. Brus, Annu. Rev. Phys. Chem. **41**, 477 (1990).
[14] A. D. Yoffe, Adv. Phys. **42**, 173 (1993).
[15] C. B. Murray, D. J. Norris, and M. G. Bawendi, J. Am. Chem. Soc. **15**, 8706 (1993).
[16] J. E. Bowen Katari, V. L. Colvin, and A. P. Alivisatos, J. Phys. Chem. **98**, 4109 (1994).
[17] M. Kuno, J. K. Lee, B. O. Dabousi, F. V. Mikulec, and M. G. Bawendi, J. Chem. Phys. **106**, 9869 (1997).
[18] J. C. deMello, H. F. Wittmann, and R. H. Friend, Adv. Mater. **9**, 230 (1997).
[19] T. C. Chiang and F. J. Himpsel, in *Landolt-Börnstein: Numerical Data and Functional Relationships in Science and Technology*, edited by A. Goldman and E.-E. Koch, Landolt-Börnstein, New Series, Group III, Vol. 23, Pt. a (Springer-Verlag, Berlin, 1989), p. 95.
[20] L. E. Brus, J. Chem. Phys. **80**, 4403 (1984).
[21] I. H. Campbell, T. W. Hagler, and D. L. Smith, Phys. Rev. Lett. **76**, 1900 (1996).
[22] S. C. Moratti, D. D. C. Bradley, R. Cervini, R. H. Friend, N. C. Greenham, and A. B. Holmes, Proc. SPIE **2144**, 108 (1994).
[23] S. V. Frolov, P. A. Lane, M. Ozaki, K. Yoshino, and Z. V. Vardeny, Chem. Phys. Lett. **286**, 21 (1998).
[24] P. F. van Hutten, H.-J. Brouwer, V. V. Krasnikov, L. Ouali, U. Stalmach, and G. Hadziioannou, Synth. Met. (to be published).
[25] G. R. Hayes, I. D. W. Samuel, and R. T. Phillips, Phys. Rev. B **54**, R8301 (1996).
[26] I. D. W. Samuel, G. Rumbles, and C. J. Collison, Phys. Rev. B **52**, R11 573 (1995).
[27] N. C. Greenham, F. Cacialli, D. D. C. Bradley, R. H. Friend, S. C. Moratti, and A. B. Holmes, in *Electrical, Optical, and Magnetic Properties of Organic Solid State Materials*, edited by A. F. Garito, A. K.-Y. Jen, C. Y.-C. Lee, and L. R. Dalton, MRS Symposia Proceedings No. 328 (Materials Research Society, Pittsburgh, 1994), p. 351.
[28] L. Smilowitz, N. S. Sariciftci, R. Wu, C. Gettinger, A. J. Heeger, and F. Wudl, Phys. Rev. B **47**, 13 835 (1993).
[29] X. Wei, Z. V. Vardeny, N. S. Sariciftci, and A. J. Heeger, Phys. Rev. B **53**, 2187 (1996).
[30] X. Wei, S. V. Frolov, and Z. V. Vardeny, Synth. Met. **78**, 295 (1996).
[31] G. Dellepiane, C. Cuniberti, D. Comoreto, G. F. Musso, and G. Figari, Phys. Rev. B **48**, 7850 (1993).
[32] N. F. Colaneri, D. D. C. Bradley, R. H. Friend, P. L. Burn, A. B. Holmes, and C. W. Spangler, Phys. Rev. B **42**, 11 670 (1990).
[33] M. P. T. Christiaans, M. M. Wienk, P. A. v. Hal, J. M. Kroon, and R. A. J. Janssen, Synth. Met. (to be published).
[34] X. Wei, B. C. Hess, Z. V. Vardeny, and F. Wudl, Phys. Rev. Lett. **68**, 666 (1992).